Natural bacterial assemblages in *Arabidopsis thaliana* tissues become more distinguishable and diverse during host development

Authors & Affiliations

Kathleen Beilsmith[a*], Matthew Perisin[a,b*], Joy Bergelson[a]

[a] Department of Ecology and Evolution, University of Chicago, 1101 E 57th St, Chicago, IL, 60637 USA

[b] Current Address: U.S. Army Combat Capabilities Development Command Army Research Laboratory, FCDD-RLS-CB, 2800 Powder Mill Rd, Adelphi, MD 20783

* These authors contributed equally to this work

Corresponding Author

Joy Bergelson, jbergels@uchicago.edu

Abstract

To study the spatial and temporal dynamics of bacterial colonization under field conditions, we planted and sampled *Arabidopsis thaliana* during two years at two Michigan sites and surveyed colonists with 16S rRNA gene amplicon sequence variants (ASVs). Mosaic and dynamic bacterial assemblages revealed the plant as a patchwork of tissue habitats that differentiated with age. ASV prevalence patterns varied not only between roots and the phyllosphere but among phyllosphere tissues. Increasing assemblage diversity indicated that variants dispersed more widely over time, decreasing the importance of stochastic variation in early colonization relative to tissue differences. As tissues underwent developmental transitions, the root and phyllosphere assemblages became more distinct. This pattern was driven by common variants rather than those restricted to a particular tissue or transiently present at one developmental stage. Patterns also depended critically on fine phylogenetic resolution: when ASVs were grouped at coarse taxonomic levels, their associations with host tissue and age disappeared. Thus, the observed spatial and temporal variation in colonization depended upon bacterial traits that were less conserved than the family-level metabolic functions recently reported to govern *ex situ* plant microbiome assembly. Some colonists were consistently more successful at entering specific tissues, as evidenced by their repeatable spatial prevalence distributions across sites and years. However, these variants did not overtake plant assemblages, which instead became more even over time. Together, these results suggested that the increasing effect of tissue type was related to colonization bottlenecks for specific ASVs rather than to their ability to dominate other colonists once established.

Importance

The efficiency with which bacteria colonize plants is an important parameter in the study of microbial community assembly and bacterial pathogenesis. We sampled roots and each emerging shoot tissue throughout an annual plant's life cycle in order to better understand where, when, and how the host influenced the bacterial portion of its microbiome in field conditions. Host plant filtering produced distinct microbiomes in roots and shoots as well as in different above-ground tissues. Mature tissue samples provided better insight into the host's role in shaping assembly since microbiome composition became more tightly linked to tissue differences, particularly between leaves and roots, as development progressed. These tissue differences disappeared at taxonomic levels higher than genus. Thus, this host effect might depend on recently acquired bacterial traits related to successful colonization of the leaf niche rather than on more deeply conserved metabolic traits.

INTRODUCTION

As plant tissues emerge and grow, new habitats are created for microbial colonists (1, 2). While they represent only a fraction of colonist diversity (3, 4), bacterial endophytes are important to host plant fitness because of their potential to affect nutrient uptake (5, 6, 7), stress responses (8), and defenses against pathogens (9, 10). Given these activities, natural and engineered bacterial communities have been proposed as tools for sustainably enhancing plant growth and stress resistance (11). When lineages in these communities are pathogenic or beneficial to the host, the efficiency with which they enter plant tissue is of particular interest (12, 13, 14). Despite stochasticity in colonization (15, 16, 17), there is evidence that plants selectively filter the bacteria colonizing the intercellular space in their tissues. Characterizing spatial and temporal variation in this filtering is key to understanding how natural and cultivated communities assemble in the endosphere.

The idea that plant tissue filters bacterial colonists is supported by the observation that endophytic communities display only a fraction of the diversity found in soil. For example, the diversity of taxa found in the root endosphere is lower than in rhizosphere soil (18). Furthermore, a subset of bacterial families is found at higher relative abundance in roots than in soil (19). Filtering is likely due in part to differences between soil and root cell walls as substrates for colonization, as indicated by similarities between communities in live roots and wood slivers exposed to the same field-collected soil inocula (20). Filtering by living tissue may also involve selection for or against specific bacterial lineages, as indicated by community members enriched over soil levels in roots but not in wood sliver samples and vice versa (20).

Although plant tissue appears to filter bacterial colonists, we do not yet fully understand how spatial and temporal variation influences this process in natural environments. Variation in abiotic factors and the pool of soil colonists at planting sites can influence the efficiency with which bacterial lineages enter plants, leading to associations between geographic location and the composition of bacterial assemblages in plant tissues (21, 22, 23). Within plants, recent evidence suggests that communities in different tissues are composed of a common pool of systemic colonists (24, 25). However, individual lineages can display differences in colonization efficiency between roots and stems (26) and several studies report variation between the bacterial assemblages found in different tissues (27, 28, 29), supporting the idea that some bacteria are more successful than others in colonizing a given habitat within the plant. Variation in assemblage composition is also observed when plant tissues are sampled at different developmental stages (22, 30, 31). These temporal trends could be related to the time available for bacterial colonization of plant tissues before sampling or to changes in how hosts filter colonists with age. Since bacteria alter plant tissues upon arrival, the host response to established colonizers could also change the efficacy of colonization later in development (32, 33).

Since most surveys of plant colonists have either focused on a single tissue or taken only a snapshot of community composition in time, it is difficult to compare the extent and interaction of geographic, tissue-level, and temporal effects on plant endophyte filtering. Adding to the body of work exploring host plant control of colonization, we compared the relative influence of plant tissue type, age, harvest site, and year on the bacteria that naturally colonized a common haplotype of an annual plant, *Arabidopsis thaliana*. To understand the conservation of the bacterial traits driving these patterns, we examined whether relationships between variables and assemblage composition depended on the taxonomic level at which the surveyed colonists were grouped. To ascertain the consistency of spatial

and temporal colonization patterns, we compared the tissues and ages at which bacterial lineages reached maximum prevalence or abundance between sites and years. In addition, we characterized how the diversity and evenness of colonists changed across plant tissues throughout development.

TABLE 1 Samples in the study after quality control (at site ME, at site WW)

	Soil	Roots	Rosettes	Stems	C. Leaves	Flowers	Siliques	Total
No Plant	15, 19							34
Two-Leaf Plant	6, 4	3, 4	8, 10					35
Four-Leaf Plant		29, 8	27, 29					93
Six-Leaf Plant	8, 4	32, 18	45, 26					133
Eight-Leaf Plant		37, 24	41, 35					137
Flowering Plant	4,3	61, 38	64, 49	41, 38	24, 22	42, 28	14, 25	453
Senescent Plant	6,8	60, 64		54, 75			49, 71	387
Total	77	378	334	208	46	70	159	1272

RESULTS

We planted surface-sterilized seeds of *A. thaliana* accessions from a single North American haplotype (Supplementary Table S1) at two southwest Michigan sites in two consecutive years. These accessions germinate in the fall, overwinter as small rosettes, flower in the spring, and senesce in the early summer. We harvested roots and rosette leaves throughout vegetative growth and also stems, cauline leaves, flowers, and siliques as they became available during flowering and senescence (Supplementary Table S2). To enrich for endophytes, bacteria were washed from the surface of plant tissues by repeated vortexing in surfactant buffer (Supplementary Methods S3). Topsoil was also collected from field sites at each timepoint during the second year of study. Bacterial lineages in the soil and plant tissue samples were quantified by amplification and sequencing of the V5, V6, and V7 regions of the 16S rRNA gene (16S) (29). The 16S sequences were grouped into amplicon sequence variants (ASVs) with DADA2 (34) in QIIME2 (35). After filtering out singleton 16S variants and those from plant organelles, 10,803 ASVs were tallied for 1,272 samples (Table 1). A phylogenetic tree for the variants was inferred with FastTree using MAFFT-aligned 16S sequences (36, 37). The ASVs were classified at seven taxonomic ranks based on the SILVA 16S database (38).

Bacterial assemblage composition was associated with plant tissue type and developmental stage.

Plants shaped the bacterial assemblages they hosted, making them distinct from those in the surrounding soil (Supplementary Text S4). Rather than a single host environment, the plant appeared to be a collection of habitats defined by tissue type and age. Samples from the same tissue or stage clearly shared a higher proportion of members than randomly compared samples (Random samples: median = 0.094; Same Tissue: median = 0.133, $p < 2.2 \times 10^{-16}$; Same Stage: median = 0.117, $p = 2.4 \times 10^{-11}$), while samples from the same site or year had increased membership overlap at lower significance thresholds (Same Site: median = 0.104, $p = 5.04 \times 10^{-4}$; Same Year: median = 0.100, p = 0.033). Despite these patterns, the low proportion of members shared within groups conditioned on any sample variable (< 15%) underscored the high variability of colonization. When samples from multiple tissues of the same individual plant were available, comparisons showed that they did not share a significantly higher proportion of members than randomly paired samples (Same Plant ID: median: 0.922, p =

0.418). Plant-associated bacterial assemblages therefore appeared to be more similar between samples of the same tissue type from different plants than between samples from different tissue habitats in the same plant.

The influence of tissue type and developmental stage on assemblage composition was further supported by analysis of variance. Composition variation between samples was quantified with the Raup-Crick dissimilarity index (39) and analysis of variance with permutation was performed on the matrix of dissimilarity indices ($\alpha = 0.001$). Variance between ecotypes ($p = 0.57$) was not greater than the variance within them, which is unsurprising given the genetic similarity of the haplogroup to which they belonged (40). Variance among plant individuals was insignificant at the designated threshold ($p = 0.02$) (Supplementary Table S5). Tissues, developmental stages, planting sites, years, sample preparation plates, and sequencing runs differed significantly in composition. These six variables were nested according to the experimental design and ordered by the proportion of variance they explained to create a multivariate model for permutational analysis of variance (PERMANOVA) (41). When PERMANOVA was performed with this model, tissue type and developmental stage were assigned 13% and 9% of the total variance in sample dissimilarities (Table 2). PERMANOVA was also performed with the term for plant individual, significant at $\alpha = 0.05$, nested within harvest stage in order to test whether that term could help explain more variance; however, it was insignificant in a multivariate model ($p = 0.494$). Regardless of the dissimilarity or distance used to quantify differences, such as Bray-Curtis (42) or unweighted UniFrac (43), assemblage composition was most strongly associated with host tissue type followed by plant age (Table 2).

Plants were composed not only of distinct root and phyllosphere niches but also of at least two distinct environments within the phyllosphere. Plant samples segregated by tissue type in principle coordinate analysis (PCoA) based on their Raup-Crick dissimilarities (Figure 1B), with the eigenvalue for the first principle coordinate accounting for 45.5% of the sample variance. Samples from the stem and silique tissues, which emerged during flowering, clustered separately from rosette leaf samples along this principle coordinate. The clustering of ordinated samples by tissue type, including within the phyllosphere, was robust to the dissimilarity or distance metric used, as well as to rarefaction, filtering, and normalization of the count data (44) (Supplementary Figure S6). Among samples of five phyllosphere tissues from flowering plants, the PERMANOVA term for plant tissue type nested within year still explained 4% of the variation in ASV presence ($p = 0.01$). When only phyllosphere samples from flowering plants were ordinated, rosette leaves and later-emerging tissues overlapped but the former clustered more tightly, revealing that the significant differences in composition within the phyllosphere were primarily between the rosette leaves and tissues emerging with inflorescence (Figure 1C).

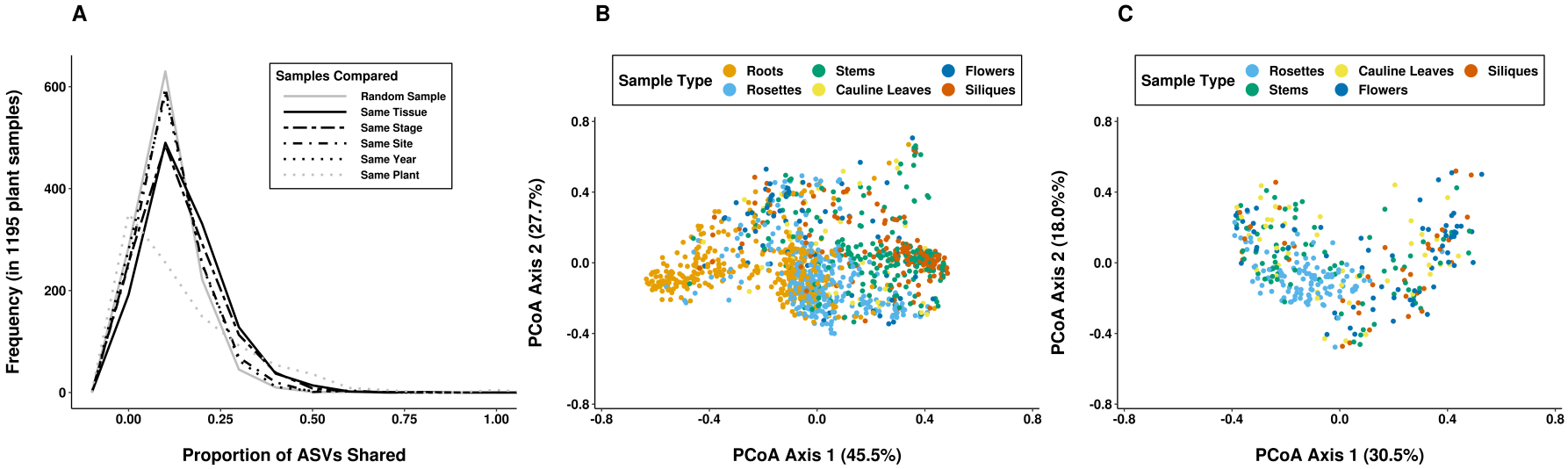

Figure 1. Bacterial assemblage composition was driven by the tissue sampled and the plant's developmental stage at harvest. (A) The frequency distribution for the proportion of ASVs shared by plant samples selected randomly (solid gray) differed from those for plant samples selected with respect to tissue type, developmental stage, site, or year (patterned black lines). The proportion of shared members was significantly higher when sample selection was conditioned on each variable, but the strongest shifts were observed for tissue type and developmental stage. The frequency distribution for the proportion of ASVs shared with any samples taken from different tissues of the same individual plant is also shown (dotted gray line). (B) Plant samples segregated by tissue type in principle coordinate analysis (PCoA) based on their Raup-Crick dissimilarities. The eigenvalue for the first principle coordinate accounted for 45.5% of the sample variance. Samples from roots (orange), rosette leaves (blue), and stems and siliques (green and red) clustered along this coordinate. (C) Phyllosphere samples at flowering were ordinated based on their Raup-Crick dissimilarities. Rosette leaves (blue) overlapped with other phyllosphere tissues but appeared to cluster more tightly.

TABLE 2 PERMANOVA results for plant samples

Raup-Crick index ~ Year / Stage / Tissue + MiSeq Run / Sample Plate + Site				1195 samples, 8271 ASVs
Variable	DOF	F	R^2	Pr (>F)
Year : Stage : **Tissue**	19	12.191	0.13119	< 0.001
Year : **Stage**	8	20.179	0.09143	< 0.001
Site	1	73.524	0.04164	< 0.001
MiSeq Run : **Sample Plate**	20	3.447	0.03904	< 0.001
Year	1	55.615	0.0315	< 0.001
MiSeq Run	3	10.827	0.0184	< 0.001
Residuals			0.6468	
Bray-Curtis dissimilarity (rarefied data) ~ Year / Stage / Tissue + MiSeq Run / Sample Plate + Site				712 samples, 5617 ASVs
Year : Stage : **Tissue**	17	6.986	0.12352	< 0.001
Year : **Stage**	7	12.096	0.08807	< 0.001
Site	1	40.251	0.04187	< 0.001
Year	1	25.201	0.02621	< 0.001
MiSeq Run : **Sample Plate**	20	1.225	0.02548	0.002
MiSeq Run	3	2.021	0.00631	< 0.001
Residuals			0.68855	
UNIFRAC distance (rarefied data) ~ Year / Stage / Tissue + MiSeq Run / Sample Plate + Site				712 samples, 5617 ASVs
Year : Stage : **Tissue**	17	7.9134	0.14332	< 0.001
Year : **Stage**	7	7.9713	0.05945	< 0.001
Miseq Run: **Sample Plate**	20	1.3908	0.02963	< 0.001
Site	1	25.4283	0.02709	< 0.001
MiSeq Run	3	5.7466	0.01837	< 0.001
Year	1	15.8517	0.01689	< 0.001
Residuals			0.70525	

Assemblages in phyllosphere tissues became more distinguishable from those in roots as plants matured.

To disentangle the roles of spatial and temporal variables in defining habitats within the plant, we compared root and shoot tissues with respect to the ASVs present both before and after developmental transitions. Roots and rosettes were compared between late vegetative and flowering stages while roots and stems were compared between flowering and senescence. Tissue assemblages grew more distinguishable later in development, with the proportion of variance explained by tissue relative to other host variables increasing at later stages (Table 3, Supplementary Table S7). The differentiation of tissue habitats over time was further examined by quantifying their β diversity at each stage in a rarefied dataset. Pairwise unweighted UniFrac distances of samples within and between tissue types were calculated and the distributions of these distances were compared for both rosette leaves and roots (Figure 2A). As development progressed, root assemblages varied as much among each other as any did from those in the phyllosphere while leaf assemblages became more similar to each other, and simultaneously more distinct from those in the roots, perhaps due to unique selective pressures in the phyllosphere. During development, the influence of site did not differ between tissue types, suggesting that the distinct compositions of root and phyllosphere assemblages did not arise because of differences in their response to the local environment (Figure 2B).

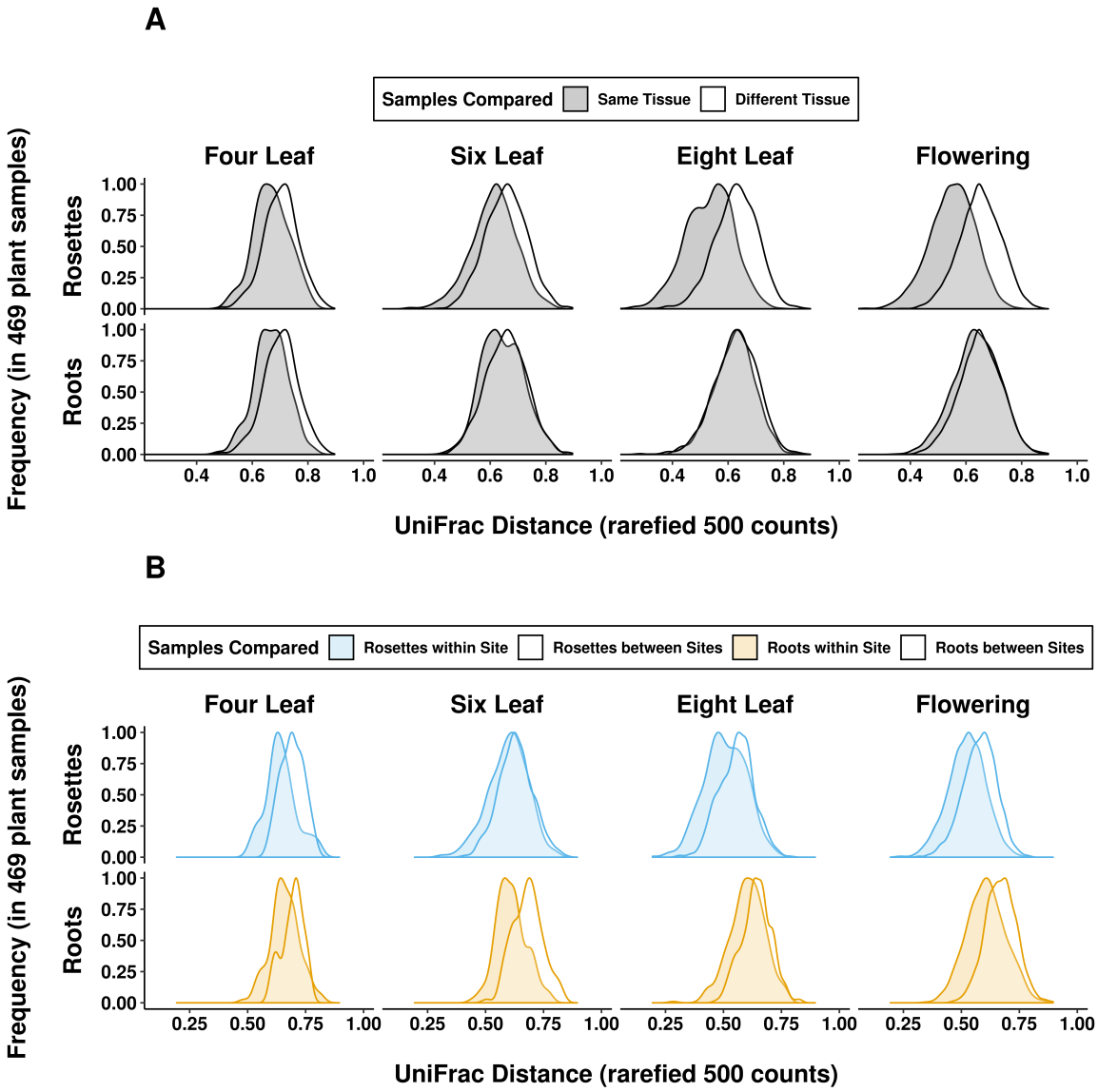

Figure 2. Phyllosphere assemblages became more uniform and distinguishable from those in roots as plants matured. The dataset was pruned to samples with at least 100 counts and 20 ASVs to calculate unweighted UniFrac distances between samples. (A) The distribution of UniFrac distances between samples within a tissue type (shaded distribution) was compared to the distribution of distances between samples from different tissue types (shaded distributions). This procedure was repeated for rosette samples (top panel) and root samples (bottom panel). As plants matured (horizontal panels left to right), root samples were consistently as distant from each other as they were from the phyllosphere. Phyllosphere samples were increasingly similar to each other and distinguishable from the root samples. (B) The distributions of UniFrac distances between samples from the same site (shaded distributions) were compared to the distributions of UniFrac distances between samples from different sites (unshaded distributions). The relationship of site to composition is visible because samples from the same sites tend to have lower UniFrac distances. However, this relationship does not appear to differ between rosette leaves (top panel) and roots (bottom panel) or over time (horizontal panels).

TABLE 3 PERMANOVA results for tissue comparisons at different stages

Comparison	ASVs	Samples	Tissue R^2 / All Variables R^2
Vegetative Roots and Rosettes	1192	258	0.278
Flowering Roots and Rosettes	1192	212	0.487
Flowering Roots and Stems	1411	177	0.435
Senescent Roots and Stems	1411	253	0.828

Assemblage associations with tissue and stage depended on sub-genus variation in bacteria.

In the study of microbiome assembly, patterns can depend upon the taxonomic resolution with which bacteria are surveyed. ASVs represent the finest resolution of bacterial lineages possible with 16S data. If the effect of host tissue type was driven by differential filtering of closely related variants rather than larger bacterial clades, then it should weaken as taxonomic resolution decreases. To determine the dependence of the observed associations on taxonomic grouping, PERMANOVA was repeated with a Raup-Crick dissimilarity matrix produced with tables of ASV counts aggregated at the level of genus, family, order, and class (Table 4, Supplementary Table S8).

Associations between assemblage composition and host tissue and age weakened with coarser taxonomic groupings of ASVs from genera to class. Since the distribution of traits in microorganisms is strongly tied to vertical inheritance (45), even in the face of horizontal gene transfer, the disappearance of associations with coarser grouping suggested that deeply conserved bacterial traits were not driving the distribution of colonists within the host. Instead, relatively recently evolved variation between the bacterial lineages played a role in their spatial and temporal distributions and, as a consequence, differences in the colonization patterns across tissues and stages is erased upon averaging the prevalence patterns of recently diverged ASVs across taxonomic groups.

TABLE 4 PERMANOVA results for plant samples with ASVs grouped by taxonomy

Taxonomic Rank	% ASVs unassigned	Tissue R^2	Tissue Pr (>F)	$p < 0.001$ with random groups (n=10)
ASV	0	0.13119	< 0.001	
Genus	43.94	0.05233	< 0.001	
Family	17.71	-0.12317	1	4
Order	8.17	0.01328	0.543	0
Class	2.97	0.05403	0.214	0

Assemblage associations with tissue and stage were driven by the same ASVs, which were neither tissue-specific or transient.

Changes in assemblage composition with plant age were driven by differential filtering of the same colonists that distinguished plant tissues within each developmental stage. By sampling different tissues at multiple timepoints, we were able to compare the bacterial lineages that distinguished assemblages across space and time. The ASVs driving the tissue association were identified as follows: Regression coefficients were extracted from the results of the PERMANOVA on Raup-Crick dissimilarities. Absolute values of the coefficients for tissue type were summed to obtain a measure of effect size for each ASV. Then, ASVs with the top 5% of effect sizes were selected. The minimum effect size for this set of tissue-discriminating ASVs was then used as a threshold for selecting the ASVs that most distinguished stages, sites, and years based on their summed regression coefficients. The relationships of host tissue type and age to assemblage composition were driven by overlapping sets of ASVs. Of the 168 ASVs driving the stage association, 166 were also among the 413 that drove the differences between tissue types.

Endophytic habitats within the plant were not differentiated by colonists restricted to one type of tissue or developmental stage. The ASVs driving tissue and stage effects generally appeared in multiple plant tissues rather than being restricted to a single habitat within the plant (94%). These tissue-discriminating and stage-discriminating ASVs were generally recurrent in a tissue throughout development rather than detected transiently at a single harvest (92%). Although they were not always highly prevalent (only 38% appeared in more than half of samples from a given tissue, stage, site, and year), they were among the most abundant members of the assemblages; in fact, 79% had an abundance above the median plus one standard deviation of the abundance distribution for all ASVs found in samples from the same tissue, stage, site, and year.

Although a small group of tissue-discriminating ASVs had consistent spatial prevalence distributions across field sites and years, most had inconsistent spatial and temporal patterns.

If tissue-specific host traits created environments favorable to particular colonists, then the spatial distributions of those colonists within the plant should be repeated across the sites and years in which they were observed. To assess whether ASV spatial distributions were repeated, the tissues in which ASVs reached maximum prevalence, when present, were compared between sites and years. Based on these comparisons, 37% of the ASVs distinguishing tissues displayed consistent spatial trends, always peaking in prevalence in the same tissues (Figure 3, Supplementary Figure S9). For this fraction of ASVs, colonization patterns might be linked to tissue-specific host traits that differentially filter bacterial colonists. Of these consistently distributed ASVs, 76% were always most prevalent within roots, 14% in rosettes, 4% in stems, and 6% in siliques. Relative abundance distributions were less consistent, as only 19% of tissue-discriminating ASVs reached their highest mean relative abundance in the same tissue across replicate sites and years. Notably, the genus *Massilia* includes two distinct sets of ASVs that differed in the tissues in which relative abundances consistently peaked; one set consistently peaked in roots and rosettes while the second consistently peaked in stems and siliques, emphasizing that sub-genus variation between bacterial lineages influenced their distributions within plants (Figure 3).

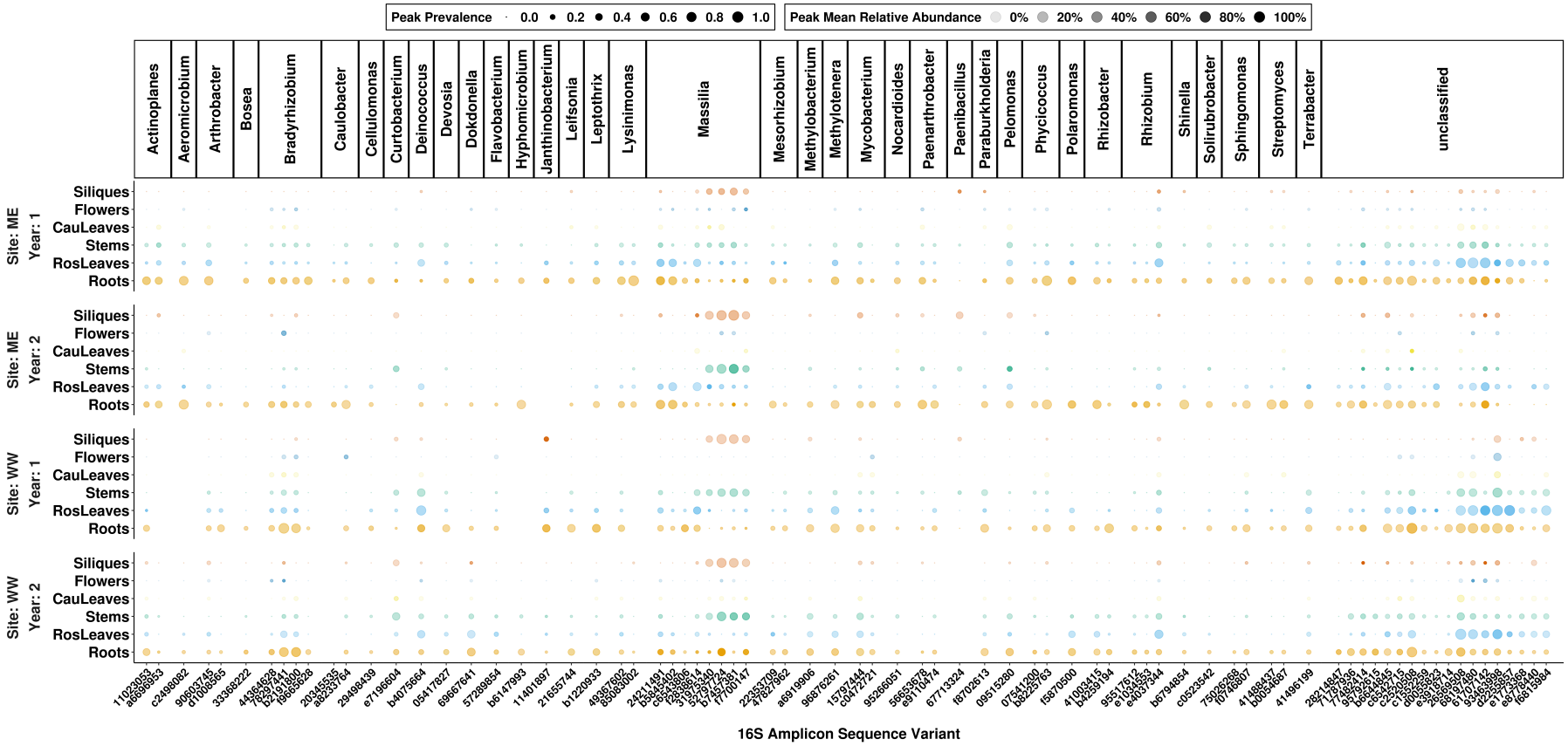

Figure 3. A fraction of tissue-discriminating ASVs behaved consistently across tissues at each site and in each year of the study. The ASVs distinguishing tissues, selected by regression coefficients, were filtered for those that reached maximum prevalence consistently in the same tissue for all the site and year combinations in which they were present. The ASVs with a total prevalence above five percent in all site and year combinations were selected for the plot. Dots represent the maximum prevalence (size) and relative abundance (saturation) for each ASV in each tissue. Panels on the y-axis separate sites and years and ASVs are grouped on the x-axis by genus. Despite the significant association detected between assemblage composition and tissue type, only 37% of ASVs consistently reached peak prevalence in the same tissue across sites and years and only 19% reached peak mean relative abundance in the same tissue across sites and years.

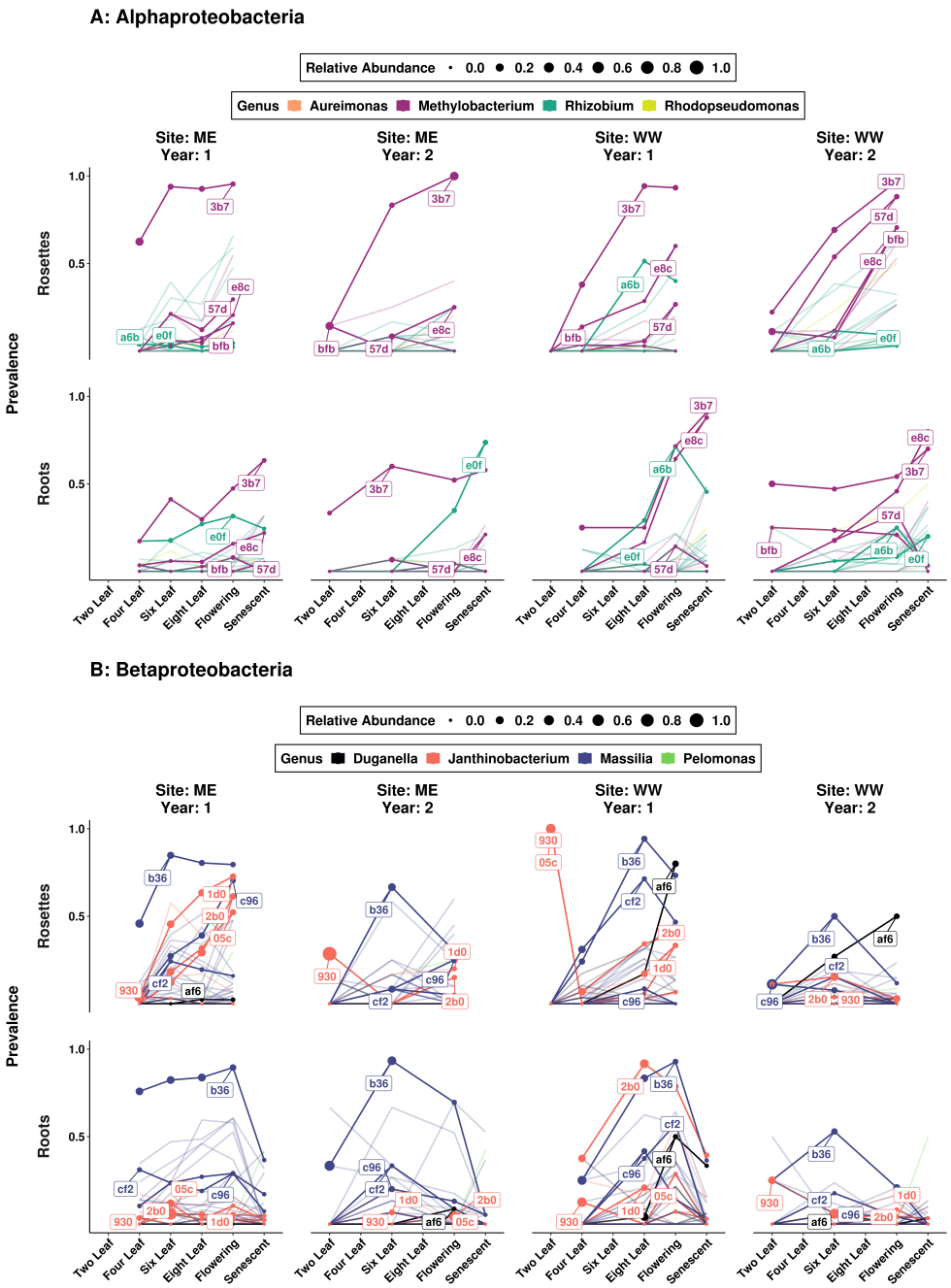

Figure 4. Most ASVs had inconsistent temporal trends in prevalence and relative abundance across sites and years. Plots show the mean prevalence (y-axis) over time for the ASVs in (A) Alphaproteobacteria and (B) Betaproteobacteria that drove the association of assemblage composition with developmental stage. ASV trends are colored by genus and panels separate the trends for roots and rosettes in each site and year. ASVs that reached over 70% prevalence in at least one panel are bolded, labeled, and include relative abundance information for each stage (point size). Temporal colonization patterns were highly inconsistent despite the detected association between composition and stage. Only 26% of ASVs consistently reached peak prevalence at the same stage across sites and years and only 14% reached peak mean relative abundance at the same stage across sites and years.

Temporal distributions also varied between sites and years for the ASVs driving associations between assemblage composition and host developmental stage. About a quarter (26%) of stage-discriminating ASVs reached maximum prevalence at the same stage in each replicate of the experiment. Changes in relative abundance were less consistent, with roughly half as many ASVs (14%) peaking at the same time across sites and years. Two exceptions show consistent prevalence patterns over time in roots and rosettes across sites and years: a *Methylobacterium* ASV (abbreviated "3b7" in Figure 4A) and a *Massilia* ASV (abbreviated "b36" in Figure 5B). Temporal distributions, like spatial ones, were typically dependent on fine taxonomic variation because ASVs within each genera displayed a variety of dynamics (Figure 4).

Assemblages became more phylogenetically diverse and even over time.

Changes in assemblage α diversity over time can help explain the increased differentiation between assemblages inhabiting different tissues. Though colonization declined as plants senesced, the bacterial variants present were more widely dispersed (that is, more prevalent) among plants. Assemblage richness, or the number of unique variants detected per gram of tissue sampled, varied between stages and ultimately decreased during senescence (Figure 5A). Despite this decrease in the density of colonists, the phylogenetic diversity of the colonists was higher later in development (Figure 5B). Phylogenetic diversity was quantified by taking the tree of 16S variants present in each assemblage, weighting the branch lengths by variant abundance, and summing the branch lengths (46). These diversity trends were observed in each type of plant tissue sampled (Supplementary Figure S10) but not in samples of the surrounding soil (Figure 5), indicating they were related to the colonization of plant tissue and not purely driven by the abiotic environment during sample collection. The increasing phylogenetic diversity suggested that bacteria from across the tree had dispersed more widely among plant assemblages later in development. With more opportunities to encounter plants over time, subtle differences in the ASV colonization success between tissues were more likely to be exposed.

Temporal trends in assemblage evenness suggested that tissue type was related to the size of the colonization bottleneck for specific ASVs rather than to their ability to dominate other colonists once established in the endosphere. Despite the influence of tissue type, variants that more frequently colonized particular tissues (Figure 3) did not overtake assemblage biomass. Variants like *Methylobacterium* "3b7" became more prevalent during development but did not dramatically increase their average relative abundance within assemblages (Figure 4). Instead of domination by a small number of successful variants, mature tissues housed, on average, a more evenly represented set of increasingly diverse ASVs. The average Shannon-Wiener index (47) of assemblages increased (Figure 5C), the median relative abundance of ASVs in the assemblages decreased (Figure 6), and the maximum relative abundance in each assemblage decreased (Figure 5D). Together, these trends showed that counts in each assemblage were distributed more evenly among ASVs at later timepoints.

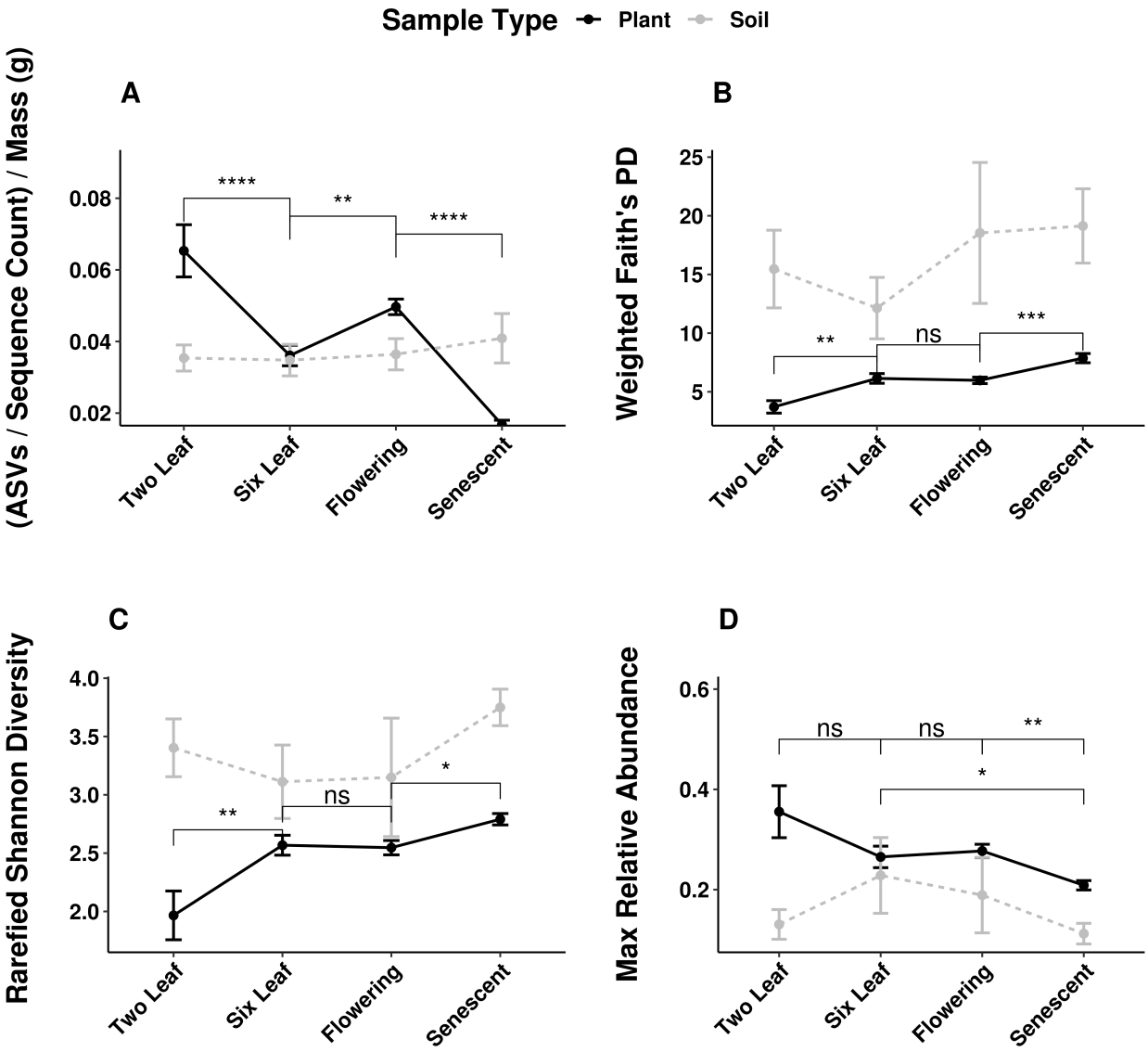

Figure 5. Assemblages within plants became more phylogenetically diverse and even over time. All plots show mean and standard error for diversity measures of the plant (black) and soil (gray) samples at each developmental stage in the second year of study. Significance is shown for pairwise Wilcoxon tests between stages as follows: ns (not significant), * ($p < 0.05$), ** ($p < 0.01$), *** ($p < 0.001$), **** ($p < 0.0001$). (A) ASV richness, or the number of ASVs in a sample, was corrected for the number of sequence counts in the sample and sample mass. The average species richness per gram of tissue differed between developmental stages and decreased overall as plants transitioned from vegetative growth to senescence. (B) Phylogenetic distance was measured as the branch length on the 16S phylogenetic tree between ASVs in the sample, weighted by ASV abundances. It increased on average with developmental stage. (C) Shannon-Wiener (H') indices from rarefied samples depended upon both the richness and evenness of samples and increased on average with developmental stage. (D) The inequality of the assemblage was represented by the maximum relative abundance of the ASVs present and it decreased on average during development.

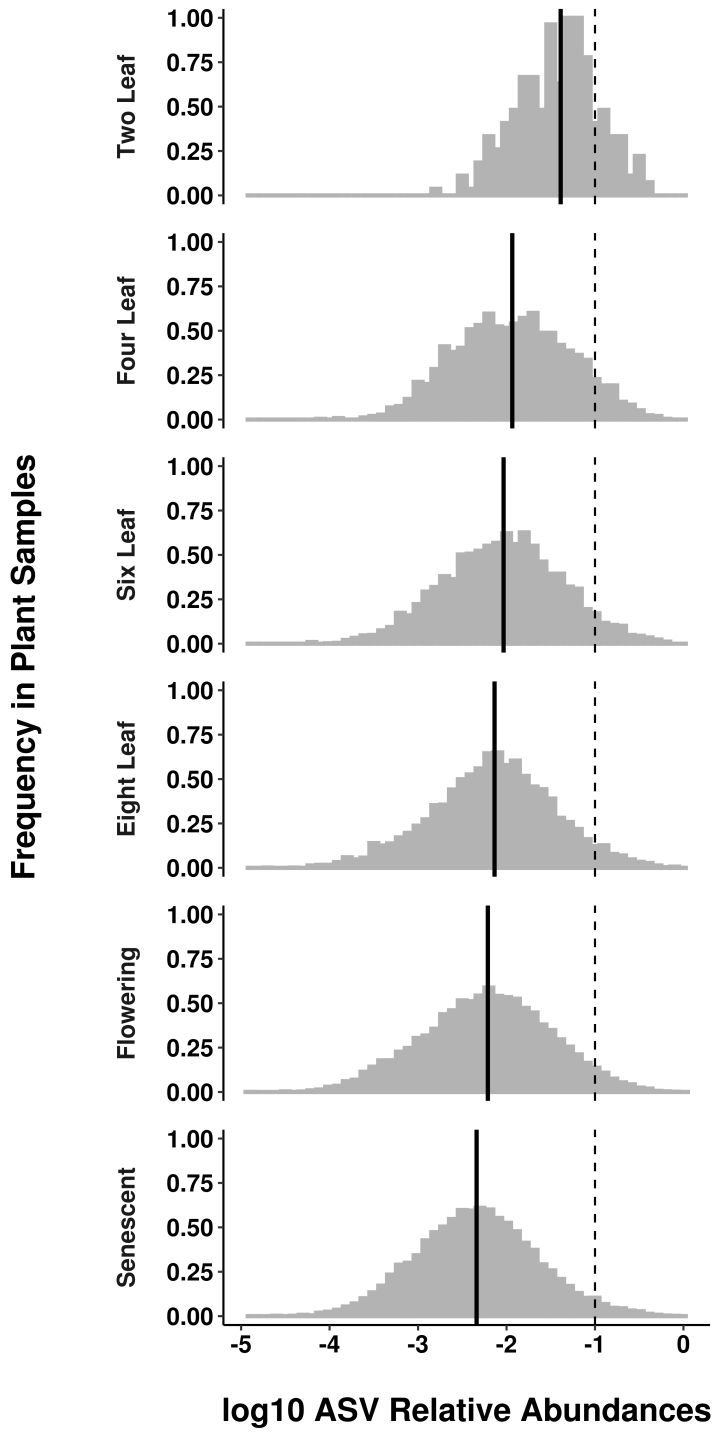

Figure 6. ASV relative abundances decrease during development as assemblages become more even. For plant samples with at least 100 counts, the realtive abundance of each ASV present was calculated. The frequency distributions of these relative abundances are plotted for each developmental stage (panel), with relative abundance scaled by log10. The solid black line represents the distribution median, which decreases as development progresses. The dashed black line represents 10% relative abundance.

DISCUSSION

We surveyed bacterial assemblages inside roots and phyllosphere tissues throughout the life cycle of the model annual plant *A. thaliana*. Consistent with previous results, we found that assemblage composition differed between tissues (29) and during the course of development (20, 30). Because we examined multiple tissues and developmental stages in the same study, we were able to find two connections between these spatial and temporal trends in colonization that have not previously been identified.

First, the associations of host tissue type and developmental stage with assemblage composition were driven by the same colonists. These bacterial variants did not constitute omnipresent cores of tissue-specific inhabitants: those most strongly associated with tissue type typically did not reach seventy-five or even fifty percent prevalence within samples from a tissue type at a given time. Nor were these variants rare: most were observed at multiple timepoints and in multiple tissues. Instead, differential filtering over space and time quantitatively affected the prevalence of common endophytes, consistent with a recent report of consistent phyllosphere organ occupancy (24).

Second, endophytic assemblages filtered by root and shoot tissues became more distinguishable later in development. Specifically, leaf assemblages grew more similar to each other and more differentiated from root assemblages on average. ASVs with consistently higher prevalence in specific tissues suggested the existence of subtle differences between variants in the probability of colonizing particular tissue niches. Increasing phylogenetic diversity indicated that bacterial lineages became more widely dispersed during plant development. As variants had more opportunities to colonize plant tissue, differences in the probability of colonizing particular tissues became more important in determining assemblage composition than the stochasticity of early colonization. Supporting this idea of the host plant gaining influence during assembly, a recent study of rice (*Oryza sativa*) roots found that microbiome composition was dynamic during vegetative growth and stabilized later in plant life (48).

Despite the growing strength of tissue effects during development, assemblages did not collapse to a few successful inhabitants of each tissue. In contrast, assemblage evenness increased in all plant tissues, agreeing with previous reports that community diversity increases as host plant tissues age (30,31). While host tissues appear to create different colonization bottlenecks for bacterial lineages, they did not appear to favor the dominance of these ASVs over others within assemblages.

These findings have consequences for the study of another key determinant of plant microbial communities: host genotype. Host genotype effects on colonization efficiency and microbiome composition are found both among angiosperm species that diverged hundreds of millions of years ago and among crop accessions that diverged through domestication within ten thousand years (19, 26, 49,50,51,52). Compositional differences in the field can even be related to polymorphisms within a plant species (4, 53). Since the variants associated with host variables are typically present throughout the plant and recurrent during development, filtering complex natural assemblages with these criteria can increase signal in the search for host polymorphisms linked to colonization success. Since tissue-associated assemblages become more distinct later in development, the host polymorphisms linked to variant prevalence or abundance might depend on which part of the plant is sampled, and when.

The effects of plant tissue type and developmental stage on assemblage composition were large compared to that of geographic site. Our results add to a growing body of evidence that the tissue sampled from a plant can explain more variation in microbial communities than geography. Studies of *A. thaliana* and *Boechera stricta* find that geographic sites and soil inocula play a substantial role in filtering plant microbial communities (20, 23). However, studies of cultivated *Agave* find that tissue explains more variation in community composition than species and site (27). Tissue type also explains more variation in epiphytic community composition than sample site in the species *S. taccada* (28). Together, these results suggest that plants are best considered as collections of distinct habitat patches for bacterial colonization.

Our experimental design, including replicate sites and study years, allowed us to characterize consistency in distributions over space and time for the variants associated with host plant features. Biotic factors that can differ between roots and the phyllosphere, like salicylic acid, have been manipulated and shown to influence community assembly in both lab and field conditions (54,55). If such deterministic factors drove the observed variation in composition, then we might expect to see bacterial endophytes with the same across-tissue spatial distributions in repeated surveys. However, only about 40% of variants were consistently more prevalent in roots than the phyllosphere or in rosettes than flowering tissues. The inconsistent behavior of most variants is perhaps not surprising given that only about 20% of variance in composition was explained by host variables, and samples typically did not share more than 15% of their colonists. This variability in the detection of endosphere colonists suggests that in nature, as in more controlled environments (17), stochastic factors drive much of community assembly.

An important factor in detecting associations between host and colonists is the resolution with which bacterial lineages are grouped in count tables. When microbes derived from natural sources, including plant leaves, are passaged outside the host in minimal media, they produce communities that are similar at the family level despite being highly variable at the level of sequence variants (56). In our study, grouping variants by family erased the observed associations with tissue type and harvest stage. Sub-genus variation between bacterial lineages thus appeared to influence their presence in different tissues. Supporting this interpretation, endophytes within the same genus had distinct spatial and temporal distributions within plants. The functions on which different tissue environments select may be conserved at a shallower phylogenetic level than the carbon metabolism traits shared by families that determined community structure in minimal media. For example, the phyllosphere presents microbes with a variety of challenges related to desiccation, toxins from other colonists, and motility (57). Adaptations known to mitigate these challenges, such as chemosensory and antimicrobial resistance genes, have occurred recently and vary at the sub-genus level in the lineages of known phyllosphere colonists (58) (59). Traits like these could lead to greater success in colonizing the leaf niche, creating phyllosphere assemblages that are more similar to each other and distant from root assemblages. As a result, closely related strains of known pathogenic, plant-beneficial, or biocontrol taxa might not establish in the same way throughout their plant hosts. Functional profiling of the bacterial assemblages may therefore be more valuable than taxonomic profiling in understanding their spatial and temporal trends within plants.

MATERIALS AND METHODS

Planting

Field experiments were replicated over two years (2012-14) at two locations: Michigan State Southwest Michigan Research and Extension Center (ME) and University of Chicago Warren Woods Ecological Field Station (WW). Prior to planting in October, fields were tilled and grids were created with bottomless plastic pots (6-12 cm across) placed 2-5 cm into the ground and 10-30 cm apart. Within each grid, seeds for seven midwestern *A. thaliana* ecotypes were sown randomly and a fraction of pots were left empty for soil sampling. Seeds were surface-sterilized with ethanol and seedlings were thinned after germination with sterilized tweezers.

Sample collection

Plant sampling order was randomized and all tools were flame-sterilized with ethanol between samples. Root and above-ground tissues were separated into sterile plastic tubes. For soil samples, sterile tubes were pushed 2-5cm into the ground. Tubes were stored at -80 C until processing. To remove loosely associated microbes, each plant sample was washed twice by vortexing with surfactant buffer (22). Plant samples were then transferred to Matrix tubes (Thermo Scientific, Waltham, MA, USA). Above-ground tissue was first separated into compartments with a scalpel and tweezers. For large tissues, only enough material was added to allow for bead homogenization. For soil, samples were put through a 2 mm sieve and ~100 mg was transferred to a Matrix tube. The tubes were randomized in 96-well racks with respect to sampling site, year, and timepoint. To dry the material, tubes were frozen to -80 C and lyophilized overnight. To powder the tissue, sterile silica beads were sealed into each tube with a SepraSeal cap (Thermo Scientific) and tubes were shaken on the 2010 Genogrinder (SPEX, Metuchen, NJ, USA) (1750 RPM, 2 min). Dry mass was recorded and up to 36 mg of material was retained per tube. All tubes were then randomized in Nunc 96-deepwell plates (Thermo Scientific) for DNA extraction.

DNA extraction

Ground material was resuspended in TES (10 mM Tris-Cl, 1 mM EDTA, 100 mM NaCl) to a concentration of 0.04 mg/µL. Material was homogenized with the Genogrinder (1750 RPM) and homogenates (240 µL) were incubated (30 min) in new plates with lysozyme solution (Epicentre, Madison, WI, USA) at a final concentration of 50 U/µL. Proteinase-K (EMD Millipore, Billerica, MA, USA) and SDS were added to final concentrations of 0.5 mg/mL and 1%, respectively. Plates were incubated at 55 C for 4 h. An equal volume of 24:1 chloroform:isoamyl alcohol was mixed by pipette in each well. Plates were centrifuged at 6600xg with the Beckman Coulter Avanti J-25 (Beckman Instruments, Munich, Germany) for 15 min at 4 C. The top aqueous layer (350 µL) was removed and added to new plates with 500 µL 100% isopropanol. Plates were inverted to mix and incubated 1h at -20 C. After centrifugation for 15 min at 4 C, isopropanol was removed and DNA pellets were washed with 500 µL 70% ethanol. Pellets were dried in a chemical hood and resuspended in TE (100 µL, 10 mM Tris-Cl, 1 mM EDTA) by shaking. After incubation on ice for 5 min, plates were centrifuged for 12 min at 4 C and supernatants diluted 10X in TE were added to new 0.5 mL plates for PCR amplification.

16S rRNA gene amplification

The V5, V6, and V7 regions of the 16S rRNA gene were amplified from each sample using the 799F and 1193R primers with Illumina MiSeq adapters, and custom pads, linkers, and barcode sequences

(60). The PCR volume was 25 µL: 1 µL of 10X diluted DNA template, 0.2 µM of each primer, 1X 5PRIME HotMasterMix (5PRIME, Gaithersburg, MD, USA), and 0.8X SBT-PAR additive (61). PCR amplification consisted of initial denaturation at 94 C for 2min, followed by 35 cycles of denaturation at 94 C for 30 s, annealing at 54.3 C for 40 s, and elongation at 68 C for 40 s, followed by a final elongation at 68 C for 7min. Each PCR was completed in triplicate, pooled, and purified with an equal volume of Axygen AxyPrep Mag PCR Clean-Up bead solution (Corning, Tewksbury, MA, USA). Amplicon concentrations were quantified by fluorimetry (QUANT-iT PicoGreen dsDNA Assay Kit, Life Technologies, Carlsbad, CA, USA) and 30 ng or a maximum of 30 µL per sample were pooled for six plates per sequencing run. Primer dimers and mitochondrial amplicons were removed by concentrating each amplicon pool 20X (Savant SPD121P SpeedVac Concentrator, Thermo Scientific) and purifying 300-700bp product with BluePippin (Sage Science, Beverly, MA, USA).

Sequence data

Amplicon pools were sequenced using the Illumina MiSeq platform and MiSeq V2 Reagent Kits (Illumina, San Diego, CA, USA) to produce paired-end 250 bp reads (MiSeq Control Software v2.5.0.5). MiSeq Reporter v2.5.1.3 demultiplexed samples and removed reads without an index or matching PhiX. Within QIIME2, cutadapt removed primers from the paired reads and DADA2 identified ASVs. Primers 799F and 1193R were used to extract reads in silico from the QIIME-SILVA 16S database. These reads were used to build a classifier using QIIME2's naive-bayes method and the sklearn algorithm was used to generate taxonomy assignments for the sequence variants. These assignments were used to filter any remaining mitochondrial and chloroplast sequences. Sequence variants with a frequency lower than 2 counts, samples with fewer than 10 reads, and samples with notes on irregularities during collection were also removed. To generate a phylogeny for the sequence variants, QIIME2 was used to align the sequences with MAFFT and to infer and root a phylogenetic tree. The tree was imported along with the DADA2-generated ASV count table, the taxonomy, and the metadata into a phyloseq (62) class in R (version 3.4.4) (63) for analysis. Count table transformations, pruning, and rarefaction were performed with phyloseq and distance matrix calculation, ordination, and PERMANOVA tests were performed with the vegan package (64). Phylogenetic analysis was performed with ape and picante (65,66). Figures and supplemental figures were produced with ggplot2, ggpubr, ggrepel, and directlabels (67,68,69,70).

SUPPLEMENTARY MATERIAL

Table S1. *Arabidopsis thaliana* ecotypes planted in the study (from the HPG-1 haplogroup)
File: KBMP2020_S1_Table.pdf

Table S2. Sample collections for the study
File: KBMP2020_S2_Table.pdf

Text S3. Supplementary Methods
File: KBMP2020_S3_SupplementaryMethods.pdf

Text S4. Plants hosted bacterial assemblages distinct from those in the surrounding soil.
File: KBMP2020_S4_SupplementaryText.pdf

Table S5. Variables tested for association with Raup-Crick dissimilarity index matrices by PERMANOVA
File: KBMP2020_S5_Table.pdf

Figure S6. Plant tissue was the variable most strongly associated with sample composition, regardless of how composition variation was quantified or how the count tables for samples were transformed or thresholded. The relationships of host tissue type and stage to community composition were visualized by principle coordinate (PCoA) ordination of the samples based on dissimilarities or distances (Figure S1). Samples clustered primarily by the material sampled regardless of the dissimilarity or distance used. (A) Unweighted UniFrac is influenced by the phylogenetic relationships of ASVs present in samples. (B) Bray-Curtis dissimilarity is based on presence-absence patterns as well as quantitative differences in ASV abundance across samples. This pattern was robust to common methods for minimizing the effects of different count totals among samples on pairwise dissimilarities, such as transforming or subsampling ASV counts. Samples were rarefied to one thousand reads before the Bray-Curtis dissimilarity was taken. Alternatively, a variance-stabilizing transformation (C) or a log transformation (D) was performed on the count table before the Bray-Curtis dissimilarity was taken. Finally, the importance of host variables relative to site and year was robust to thresholding the ASV count table based on the prevalence or abundance. (E) ASVs were filtered for prevalence to include only those presence in more than three samples. (F) ASVs were filtered for abundance to include only those with a count total exceeding one thousand for all samples.
File: KBMP2020_S6_Figure.pdf

Table S7. PERMANOVA results for tissue comparisons at different stages
File: KBMP2020_S7_Table.pdf

Table S8. PERMANOVA results for plant samples with ASVs grouped by taxonomy
File: KBMP2020_S8_Table.pdf

Figure S9. Most tissue-discriminating ASVs had variable spatial distributions of prevalence and relative abundance between study sites and years. The ASVs distinguishing tissues were filtered for those that did not peak consistently in the same tissue across sites and years when they were present (63%). ASVs with regression coefficients for tissue type among the top 50 and a total prevalence above five percent in all site and year combinations were selected for the plot. Dots represent the maximum prevalence (size) and relative abundance (saturation) for each ASV in each tissue. Panels on the y-axis separate sites and years and ASVs are grouped on the x-axis by genus.
File: KBMP2020_S9_Figure.pdf

Figure S10. Diversity and evenness increased during development in all plant tissues. All plots show mean and standard error for diversity measures of the plant samples at each developmental stage in the second year of study. Flower and cauline leaves were only sampled at one developmental stage and thus do not have trend lines. (A) ASV richness, or the number of ASVs in a sample, was corrected for the number of sequence counts in the sample and sample mass. The average species richness per gram of tissue decreased overall as plants transitioned from vegetative growth to senescence. (B) Phylogenetic distance was measured as the branch length on the 16S phylogenetic tree between ASVs in the sample, weighted by ASV abundances. It increased on average with developmental stage. (C) Shannon-Wiener (H') indices from rarefied samples depended upon both the richness and evenness of

samples and increased on average with developmental stage. (D) The inequality of the assemblage was represented by the maximum relative abundance of the ASVs present and it decreased on average during development.
File: KBMP2020_S10_Figure.pdf

Data Availability
Raw sequencing data is available in the NCBI's Sequence Read Archive, BioProject ID PRJNA607544. The ASV count table, 16S phylogenetic tree and taxonomy, and sample metadata are available with the R commands used for analysis here: https://github.com/krbeilsmith/KBMP2020_Microbes

Acknowledgements
KB and MP were supported by the University of Chicago Biological Sciences Division and by NIH T32 GM07197. MP was supported by a Department of Education GAANN grant in ecology to Cathy Pfister. Research was supported by NIH grant R01 GM083068 to JB. Computing resources were provided by The Center for Research Informatics, funded by the Biological Sciences Division at the University of Chicago with additional funding provided by the Institute for Translational Medicine, CTSA grant number UL1 TR000430 from the National Institutes of Health.

We thank Dave Francis at the Michigan State Southwest Michigan Research and Extension Center for providing and prepping field plots. We thank Carlos Sahagun for assisting with planting and Timothy Morton, Benjamin Brachi, Talia Karasov, Manfred Ruddat, and Roderick Woolley for assistance with sampling. The DNA extraction and 16S amplicon sequencing protocols were developed in collaboration with Benjamin Brachi and Alison Anastasio provided experimental design advice. Members of the Bergelson lab and the Department of Ecology and Evolution at the University of Chicago, in particular Caroline Oldstone-Jackson and Brooke Weigel, provided valuable feedback during the data processing and analysis.

References (in order of appearance)

(1) Hardoim PR, van Overbeek LS, Berg G, Pirttilä AM, Compant S, Campisano A, Döring M, Sessitsch A. 2015. The Hidden World within Plants: Ecological and Evolutionary Considerations for Defining Functioning of Microbial Endophytes. *Microbiol Mol Biol Rev*. 79(3):293-320. doi: 10.1128/MMBR.00050-14. PubMed PMID: 26136581; PubMed Central PMCID: PMC4488371.

(2) Khare E, Mishra J, Arora NK. 2018. Multifaceted Interactions Between Endophytes and Plant: Developments and Prospects. *Front Microbiol*. 9:2732. doi: 10.3389/fmicb.2018.02732. PubMed PMID: 30498482; PubMed Central PMCID: PMC6249440.

(3) Kowalchuk, G. A., Yergeau, E., Leveau, J. H., Sessitsch, A., Bailey, M., & Liu, W. 2010. Plant-associated microbial communities. *Environmental molecular microbiology*, 131-148.

(4) Bergelson, Joy, Jana Mittelstrass, and Matthew W. Horton. "Characterizing both bacteria and fungi improves understanding of the Arabidopsis root microbiome." *Scientific reports* 9, no. 1 (2019): 24.

(5) Hilda Rodríguez, Reynaldo Fraga,. 1999. Phosphate solubilizing bacteria and their role in plant growth promotion. *Biotechnol Adv.* 17(4–5): 319-339. doi: 10.1016/S0734-9750(99)00014-2. PubMed PMID: 14538133.

(6) Franche, C., Lindström, K., & Elmerich, C. 2009. Nitrogen-fixing bacteria associated with leguminous and non-leguminous plants. *Plant and soil*, *321*(1-2), 35-59. doi: 10.1007/s11104-008-9833-8.

(7) Marulanda, A., Azcón, R., Chaumont, F., Ruiz-Lozano, J. M., & Aroca, R. 2010. Regulation of plasma membrane aquaporins by inoculation with a Bacillus megaterium strain in maize (Zea mays L.) plants under unstressed and salt-stressed conditions. *Planta*, *232*(2), 533-543. doi: 10.1007/s00425-010-1196-8.

(8) Fernandez, Olivier, Andreas Theocharis, Sophie Bordiec, Regina Feil, Lucile Jacquens, Christophe Clément, Florence Fontaine, and Essaid Ait Barka. 2012. Burkholderia phytofirmans PsJN acclimates grapevine to cold by modulating carbohydrate metabolism. *Molecular Plant-Microbe Interactions* 25(4): 496-504.

(9) Mercado-Blanco, Jesús, Dolores Rodrıguez-Jurado, Ana Hervás, and Rafael M. Jiménez-Dıaz. 2004. Suppression of Verticillium wilt in olive planting stocks by root-associated fluorescent Pseudomonas spp. Biological Control 30(2): 474-486.

(10) Kloepper, Joseph W., and Choong-Min Ryu. 2006. Bacterial endophytes as elicitors of induced systemic resistance. In Microbial root endophytes, pp. 33-52. Springer, Berlin, Heidelberg, 2006.

(11) Berg, G., Köberl, M., Rybakova, D., Müller, H., Grosch, R. and Smalla, K. 2017. Plant microbial diversity is suggested as the key to future biocontrol and health trends. FEMS microbiology ecology, 93(5).

(12) Laine, A.L. and Hanski, I., 2006. Large-scale spatial dynamics of a specialist plant pathogen in a fragmented landscape. Journal of Ecology, 94(1), pp.217-226.

(13) Kuiper, I., Bloemberg, G.V. and Lugtenberg, B.J., 2001. Selection of a plant-bacterium pair as a novel tool for rhizostimulation of polycyclic aromatic hydrocarbon-degrading bacteria. Molecular Plant-Microbe Interactions, 14(10), pp.1197-1205.

(14) Silva, H.S.A., Romeiro, R.D.S. and Mounteer, A., 2003. Development of a root colonization bioassay for rapid screening of rhizobacteria for potential biocontrol agents. Journal of Phytopathology, 151(1), pp.42-46.

(15) Obadia, B., Güvener, Z.T., Zhang, V., Ceja-Navarro, J.A., Brodie, E.L., William, W.J. and Ludington, W.B., 2017. Probabilistic invasion underlies natural gut microbiome stability. Current Biology, 27(13), pp.1999-2006.

(16) Lazzaro, B.P. and Fox, G.M., 2017. Host–Microbe Interactions: Winning the Colonization Lottery. Current Biology, 27(13), pp.R642-R644.

(17) Maignien, L., DeForce, E.A., Chafee, M.E., Eren, A.M. and Simmons, S.L., 2014. Ecological succession and stochastic variation in the assembly of Arabidopsis thaliana phyllosphere communities. MBio, 5(1), pp.e00682-13.

(18) Fitzpatrick, C. R., Copeland, J., Wang, P. W., Guttman, D. S., Kotanen, P. M., & Johnson, M. T. 2018. Assembly and ecological function of the root microbiome across angiosperm plant species. *Proceedings of the National Academy of Sciences*, *115*(6), E1157-E1165.

(19) Bulgarelli D, Garrido-Oter R, Münch PC, Weiman A, Dröge J, Pan Y, McHardy AC, Schulze-Lefert P. 2015. Structure and function of the bacterial root microbiota in wild and domesticated barley. *Cell Host Microbe*. 17(3):392-403. doi: 10.1016/j.chom.2015.01.011. PubMed PMID: 25732064; PubMed Central PMCID: PMC4362959.

(20) Bulgarelli, D., Rott, M., Schlaeppi, K., van Themaat, E. V. L., Ahmadinejad, N., Assenza, F., ... & Peplies, J. 2012. Revealing structure and assembly cues for Arabidopsis root-inhabiting bacterial microbiota. *Nature*, *488*(7409), 91.

(21) Mighell, K., Saltonstall, K., Turner, B.L., Espinosa-Tasón, J. and Van Bael, S.A., 2019. Abiotic and biotic drivers of endosymbiont community assembly in Jatropha curcas. *Ecosphere*, *10*(11).

(22) Lundberg, D.S., Lebeis, S.L., Paredes, S.H., Yourstone, S., Gehring, J., Malfatti, S., Tremblay, J., Engelbrektson, A., Kunin, V., Del Rio, T.G. and Edgar, R.C. 2012. Defining the core Arabidopsis thaliana root microbiome. *Nature*, *488*(7409), p.86.

(23) Wagner, M. R., Lundberg, D. S., Tijana, G., Tringe, S. G., Dangl, J. L., & Mitchell-Olds, T. 2016. Host genotype and age shape the leaf and root microbiomes of a wild perennial plant. *Nature Communications*, *7*, 12151.

(24) Massoni, J., Bortfeld-Miller, M., Jardillier, L., Salazar, G., Sunagawa, S. and Vorholt, J.A., 2019. Consistent host and organ occupancy of phyllosphere bacteria in a community of wild herbaceous plant species. *The ISME Journal*, pp.1-14.
(25) Grady, K.L., Sorensen, J.W., Stopnisek, N., Guittar, J. and Shade, A., 2019. Assembly and seasonality of core phyllosphere microbiota on perennial biofuel crops. *bioRxiv*, p.446369.

(26) Germaine, K., Keogh, E., Garcia-Cabellos, G., Borremans, B., Van Der Lelie, D., Barac, T., Oeyen, L., Vangronsveld, J., Moore, F.P., Moore, E.R. and Campbell, C.D., 2004. Colonisation of poplar trees by gfp expressing bacterial endophytes. *FEMS Microbiology Ecology*, *48*(1), pp.109-118.

(27) Coleman-Derr, D., Desgarennes, D., Fonseca-Garcia, C., Gross, S., Clingenpeel, S., Woyke, T., North, G., Visel, A., Partida-Martinez, L.P. and Tringe, S.G. 2016. Plant compartment and biogeography affect microbiome composition in cultivated and native Agave species. *New Phytologist*, *209*(2), pp.798-811.

(28) Amend, A.S., Cobian, G.M., Laruson, A.J., Remple, K., Tucker, S.J., Poff, K.E., Antaky, C., Boraks, A., Jones, C.A., Kuehu, D. and Lensing, B.R. 2019. Phytobiomes are compositionally nested from the ground up. *PeerJ*, *7*, p.e6609.

(29) Bodenhausen, N., Horton, M. W., & Bergelson, J. 2013. Bacterial communities associated with the leaves and the roots of Arabidopsis thaliana. *PloS one*, *8*(2), e56329.

(30) Chaparro, J. M., Badri, D. V., & Vivanco, J. M. (2014). Rhizosphere microbiome assemblage is affected by plant development. *The ISME journal*, *8*(4), 790.

(31) Leff, J. W., Del Tredici, P., Friedman, W. E., & Fierer, N. (2015). Spatial structuring of bacterial communities within individual Ginkgo biloba trees. *Environmental Microbiology*, *17*(7), 2352-2361.

(32) Beattie, G.A. and Lindow, S.E., 1999. Bacterial colonization of leaves: a spectrum of strategies. *Phytopathology*, *89*(5), pp.353-359.

(33) Brandl, M.T. and Lindow, S.E., 1998. Contribution of indole-3-acetic acid production to the epiphytic fitness of Erwinia herbicola. *Appl. Environ. Microbiol.*, *64*(9), pp.3256-3263.

(34) Callahan, B. J., McMurdie, P. J., Rosen, M. J., Han, A. W., Johnson, A. J. A., & Holmes, S. P. (2016). DADA2: high-resolution sample inference from Illumina amplicon data. *Nature methods*, *13*(7), 581.

(35) Bolyen E, Rideout JR, Dillon MR, Bokulich NA, Abnet C, Al-Ghalith GA, Alexander H, Alm EJ, Arumugam M, Asnicar F, Bai Y, Bisanz JE, Bittinger K, Brejnrod A, Brislawn CJ, Brown CT, Callahan BJ, Caraballo-Rodríguez AM, Chase J, Cope E, Da Silva R, Dorrestein PC, Douglas GM, Durall DM, Duvallet C, Edwardson CF, Ernst M, Estaki M, Fouquier J, Gauglitz JM, Gibson DL, Gonzalez A, Gorlick K, Guo J, Hillmann B, Holmes S, Holste H, Huttenhower C, Huttley G, Janssen S, Jarmusch AK, Jiang L, Kaehler B, Kang KB, Keefe CR, Keim P, Kelley ST, Knights D, Koester I, Kosciolek T, Kreps J, Langille MG, Lee J, Ley R, Liu Y, Loftfield E, Lozupone C, Maher M, Marotz C, Martin BD, McDonald D, McIver LJ, Melnik AV, Metcalf JL, Morgan SC, Morton J, Naimey AT, Navas-Molina JA, Nothias LF, Orchanian SB, Pearson T, Peoples SL, Petras D, Preuss ML, Pruesse E, Rasmussen LB, Rivers A, Robeson, II MS, Rosenthal P, Segata N, Shaffer M, Shiffer A, Sinha R, Song SJ, Spear JR, Swafford AD, Thompson LR, Torres PJ, Trinh P, Tripathi A, Turnbaugh PJ, Ul-Hasan S, van der Hooft JJ, Vargas F, Vázquez-Baeza Y, Vogtmann E, von Hippel M, Walters W, Wan Y, Wang M, Warren J, Weber KC, Williamson CH, Willis AD, Xu ZZ, Zaneveld JR, Zhang Y, Zhu Q, Knight R, Caporaso JG. 2018. QIIME 2: Reproducible, interactive, scalable, and extensible microbiome data science. 6:e27295v2 https://doi.org/10.7287/peerj.preprints.27295v2

(36) Price, M. N., Dehal, P. S., & Arkin, A. P. (2010). FastTree 2–approximately maximum-likelihood trees for large alignments. PloS one, 5(3), e9490.

(37) Katoh, K., & Standley, D. M. (2013). MAFFT multiple sequence alignment software version 7: improvements in performance and usability. Molecular biology and evolution, 30(4), 772-780.

(38) Quast, C., Pruesse, E., Yilmaz, P., Gerken, J., Schweer, T., Yarza, P., ... & Glöckner, F. O. (2012). The SILVA ribosomal RNA gene database project: improved data processing and web-based tools. Nucleic acids research, 41(D1), D590-D596.

(39) Raup, D. M., & Crick, R. E. (1979). Measurement of faunal similarity in paleontology. Journal of Paleontology, 1213-1227.

(40) Exposito-Alonso, M., Becker, C., Schuenemann, V.J., Reiter, E., Setzer, C., Slovak, R., Brachi, B., Hagmann, J., Grimm, D.G., Chen, J. and Busch, W., 2018. The rate and potential relevance of new mutations in a colonizing plant lineage. *PLoS genetics*, *14*(2), p.e1007155.

(41) Anderson, M. J. (2014). Permutational multivariate analysis of variance (PERMANOVA). Wiley statsref: statistics reference online, 1-15.

(42) Bray, J. R., & Curtis, J. T. (1957). An ordination of the upland forest communities of southern Wisconsin. Ecological monographs, 27(4), 325-349.

(43) Lozupone, C., & Knight, R. (2005). UniFrac: a new phylogenetic method for comparing microbial communities. Appl. Environ. Microbiol., 71(12), 8228-8235.

(44) Weiss, S., Xu, Z.Z., Peddada, S., Amir, A., Bittinger, K., Gonzalez, A., Lozupone, C., Zaneveld, J.R., Vázquez-Baeza, Y., Birmingham, A. and Hyde, E.R., 2017. Normalization and microbial differential abundance strategies depend upon data characteristics. Microbiome, 5(1), p.27.

(45) Martiny, A.C., Treseder, K. and Pusch, G., 2013. Phylogenetic conservatism of functional traits in microorganisms. The ISME journal, 7(4), pp.830-838.

(46) McCoy, C. O., & Matsen IV, F. A. (2013). Abundance-weighted phylogenetic diversity measures distinguish microbial community states and are robust to sampling depth. PeerJ, 1, e157.

(47) Shannon, C. E. (1948). A mathematical theory of communication. Bell system technical journal, 27(3), 379-423.

(48) Edwards, J.A., Santos-Medellín, C.M., Liechty, Z.S., Nguyen, B., Lurie, E., Eason, S., Phillips, G. and Sundaresan, V., 2018. Compositional shifts in root-associated bacterial and archaeal microbiota track the plant life cycle in field-grown rice. PLoS biology, 16(2), p.e2003862.

(49) Kembel, S. W., O'Connor, T. K., Arnold, H. K., Hubbell, S. P., Wright, S. J., & Green, J. L. 2014. Relationships between phyllosphere bacterial communities and plant functional traits in a neotropical forest. Proceedings of the National Academy of Sciences, 111(38), 13715-13720.

(50) Laforest-Lapointe, I., Messier, C., & Kembel, S. W. 2016. Tree phyllosphere bacterial communities: exploring the magnitude of intra-and inter-individual variation among host species. PeerJ, 4, e2367.

(51) Peiffer, J.A., Spor, A., Koren, O., Jin, Z., Tringe, S.G., Dangl, J.L., Buckler, E.S. and Ley, R.E. 2013. Diversity and heritability of the maize rhizosphere microbiome under field conditions. Proceedings of the National Academy of Sciences, 110(16), pp.6548-6553.

(52) Barak, J.D., Kramer, L.C. and Hao, L.Y., 2011. Colonization of tomato plants by Salmonella enterica is cultivar dependent, and type 1 trichomes are preferred colonization sites. Appl. Environ. Microbiol., 77(2), pp.498-504.

(53) Horton, M.W., Bodenhausen, N., Beilsmith, K., Meng, D., Muegge, B.D., Subramanian, S., Vetter, M.M., Vilhjálmsson, B.J., Nordborg, M., Gordon, J.I. and Bergelson, J. 2014. Genome-wide association study of Arabidopsis thaliana leaf microbial community. Nature Communications, 5, p.5320.

(54) Lebeis, S.L., Paredes, S.H., Lundberg, D.S., Breakfield, N., Gehring, J., McDonald, M., Malfatti, S., Del Rio, T.G., Jones, C.D., Tringe, S.G. and Dangl, J.L. 2015. Salicylic acid modulates colonization of the root microbiome by specific bacterial taxa. *Science*, *349* (6250), pp.860-864.

(55) Traw, M.B., Kniskern, J.M. and Bergelson, J., 2007. SAR increases fitness of Arabidopsis thaliana in the presence of natural bacterial pathogens. *Evolution: International Journal of Organic Evolution*, *61*(10), pp.2444-2449.

(56) Goldford, J.E., Lu, N., Bajić, D., Estrela, S., Tikhonov, M., Sanchez-Gorostiaga, A., Segrè, D., Mehta, P. and Sanchez, A., 2018. Emergent simplicity in microbial community assembly. *Science*, *361*(6401), pp.469-474.

(57) Vorholt, J.A., 2012. Microbial life in the phyllosphere. *Nature Reviews Microbiology*, *10*(12), pp.828-840.

(58) Clarke, C.R., Hayes, B.W., Runde, B.J., Markel, E., Swingle, B.M. and Vinatzer, B.A., 2016. Comparative genomics of Pseudomonas syringae pathovar tomato reveals novel chemotaxis pathways associated with motility and plant pathogenicity. *PeerJ*, *4*, p.e2570.

(59) Hwang, M.S., Morgan, R.L., Sarkar, S.F., Wang, P.W. and Guttman, D.S., 2005. Phylogenetic characterization of virulence and resistance phenotypes of Pseudomonas syringae. *Appl. Environ. Microbiol.*, *71*(9), pp.5182-5191.

(60) Kozich, J.J., Westcott, S.L., Baxter, N.T., Highlander, S.K. and Schloss, P.D., 2013. Development of a dual-index sequencing strategy and curation pipeline for analyzing amplicon sequence data on the MiSeq Illumina sequencing platform. *Appl. Environ. Microbiol.*, *79*(17), pp.5112-5120.

(61) Samarakoon, T., Wang, S.Y. and Alford, M.H., 2013. Enhancing PCR amplification of DNA from recalcitrant plant specimens using a trehalose-based additive. *Applications in Plant Sciences*, *1*(1), p.1200236.

(62) R Core Team (2018). R: A language and environment for statistical computing. R Foundation for Statistical Computing, Vienna, Austria. https://www.R-project.org/.

(63) phyloseq: An R package for reproducible interactive analysis and graphics of microbiome census data. Paul J. McMurdie and Susan Holmes (2013) PLoS ONE 8(4):e61217.

(64) Jari Oksanen, F. Guillaume Blanchet, Michael Friendly, Roeland Kindt, Pierre Legendre, Dan McGlinn, Peter R. Minchin, R. B. O'Hara, Gavin L. Simpson, Peter Solymos, M. Henry H. Stevens, Eduard Szoecs and Helene Wagner (2017). vegan: Community Ecology Package. R package version 2.4-5. https://CRAN.R-project.org/package=vegan

(65) Paradis, E. and Schliep, K., 2018. ape 5.0: an environment for modern phylogenetics and evolutionary analyses in R. *Bioinformatics*, *35*(3), pp.526-528.

(66) S.W. Kembel, P.D. Cowan, M.R. Helmus, W.K. Cornwell, H. Morlon, D.D. Ackerly, S.P. Blomberg, and C.O. Webb. 2010. Picante: R tools for integrating phylogenies and ecology. Bioinformatics 26:1463-1464.

(67) H. Wickham. ggplot2: Elegant Graphics for Data Analysis. Springer-Verlag New York, 2016.

(68) Alboukadel Kassambara (2018). ggpubr: 'ggplot2' Based Publication Ready Plots. R package version 0.1.8. https://CRAN.R-project.org/package=ggpubr

(69) Kamil Slowikowski (2018). ggrepel: Automatically Position Non-Overlapping Text Labels with 'ggplot2'. R package version 0.8.0. https://CRAN.R-project.org/package=ggrepel

(70) Toby Dylan Hocking (2018). directlabels: Direct Labels for Multicolor Plots. R package version 2018.05.22. https://CRAN.R-project.org/package=directlabels